



Design, synthesis, and evaluation of different scaffold derivatives against NS2B-NS3 protease of dengue virus

Lata R. Ganji¹ · Lekha Gandhi² · Venkataramana Musturi² · Meena A. Kanyalkar¹

Received: 17 June 2020 / Accepted: 27 October 2020
© Springer Science+Business Media, LLC, part of Springer Nature 2020

Abstract

The number of deaths or critical health issues is a threat in the infection caused by Dengue virus, which complicates the situation, as only symptomatic treatment is the current solution. In this regard we have targeted the dengue protease NS2B-NS3 that is responsible for the replication. The series was designed with the help of molecular modeling approach using docking protocols. The series comprised of different scaffolds viz. cinnamic acid analogs (CA1–CA11), chalcone (C1–C10) and their molecular hybrids (Lik1–Lik10), analogs of benzimidazole (BZ1–BZ5), mercaptobenzimidazole (BS1–BS4), and phenylsulfanylmethylbenzimidazole (PS1–PS4). Virtual screening of various natural phytoconstituents was employed to determine the interactions of designed analogs with the residues of catalytic triad in the active site of NS2B-NS3. We have further synthesized the selected leads. The synthesized analogs were evaluated for the cytotoxicity and NS2B-NS3 protease inhibition activity and compared with known anti-dengue natural phytoconstituent quercetin as the standard. CA2, BZ1, and BS2 were found to be more potent and efficacious than the standard quercetin as evident from the protease inhibition assay.

Keywords Dengue virus · NS2B-NS3 protease · Molecular modeling · Protease inhibition

Introduction

Dengue virus (DENV) is categorized as a pandemic, affecting most of the population in India and the globe. DENV belongs to *Flaviviridae* and the infection is transmitted by mosquitoes' specifically *A. aegypti*. DENV exists in five different serotypes (DENV 1–5) [1] and protection against all these types is a real challenge. DENV consists of positive single-stranded RNA virus that encodes a polyprotein with ten viral proteins, out of which three are structural (cap, envelope and membrane) and seven are nonstructural (NS1, NS2A, NS2B, NS3, NS4A, NS4B, and NS5).

Several scientists targeted some of the above vital DENV proteins generating important synthetic leads with variable degree of antiviral activity. Similarly, some natural phytoconstituents are reported as potential anti-DENV agents. Among all the targets available, NS2B-NS3 is considered as an important target of DENV. NS3 protease is associated with co-factor NS2B via a Gly-Ser linker, together believed to be involved in the DENV replication activity. NS3 is a trypsin-like serine protease and composed of two domains, N-terminal and C-terminal, consisting together of 618 amino acids. The N-terminal known as protease domain, consists of 1–180 residues whereas C-terminal is known as helicase domain with 180–618 residues. Although, NS3 with NS2B is believed to be responsible for the activity but the catalytic triad (His51, Asp75, and Ser135) is located in the NS3 protease domain [2–4]. It is reported that, only a part of NS2B is known to be important for NS2B-NS3 protease activity. Molecules that directly or indirectly inhibit this protease activity can hinder DENV infection. In India, during recent outbreak, Carica papaya leaves extract emerged as one of the therapeutic options and is believed to increase the platelet count in dengue-infected patients [5, 6]. The chief constituents of papaya leaves extract include quercetin (i), caffeic acid (ii), p-coumeric acid (iii), kaempferol (iv),

Supplementary information The online version of this article (<https://doi.org/10.1007/s00044-020-02660-y>) contains supplementary material, which is available to authorized users.

✉ Meena A. Kanyalkar
meenatul@gmail.com

¹ Department of Pharmaceutical Chemistry, Prin. K. M. Kundnani College of Pharmacy, Plot 23, Jote Joy Building Rambhau Salgaonkar Marg, Cuffe Parade, Mumbai 400005, India

² Department of Biotechnology and Bioinformatics, School of Life Sciences, University of Hyderabad, Hyderabad, Telangana, India

protocatechic acid (v), chlorogenic acid (vi), and 5, 7-dimethoxy coumarin (vii). Other phytoconstituents considered are baicalein (viii), fistein (ix), hyperoside (x), glabranine (xi), 7-O-methyl glabranine (xii), panduratin A (xiii), and 4-hydroxy panduratin A (xiv) indicated in Fig. 1a. We have also designed new leads from other synthetic scaffolds that are reported to have inhibitory activity against DENV viz. benzthiazole, benzimidazole, and thioguanine derivatives (H [7, 8]) depicted in Fig. 1b. Consequently, considering the structural features of these scaffolds (Fig. 1c) used in designing the new series based on natural and synthetic compounds, can further help to generate synthetic lead that can inhibit DENV.

We have used molecular docking approach for virtual screening of potential candidate molecules in NS2B-NS3 protease (PDB code: 2FOM) to get an insight toward its binding interactions with the important residues of the enzyme. In NS2B-NS3 protease complex, NS3 consists of the catalytic triad of Ser135-His51-Asp75 [9]. Apart from this triad, Gly151, Gly153, and Tyr161 are also reported as important residues. If the inhibitor interacts with any or all of these residues, they are believed to have the potential activity toward dengue. In this view, we have designed few scaffolds based on natural phytoconstituents that are analogs of caffeic acid and chalcone along with molecular hybrids of both. Likewise, we have designed analogs of benzimidazole and mercaptobenzimidazole as well. For docking protocol, as the selected crystal structure of protein was devoid of any co-crystallized ligand, we have constructed the structure of NS2B-NS3 protease complexed with an inhibitor using homology modeling approach. The crystal structure of NS2B-NS3 protease from West Nile virus (PDB code: 2FP7) [10] was found to be suitable for this purpose. It belongs to the same family as that of DENV and shares the structural similarity of catalytic triad and is available in complex with the inhibitor tetrapeptide Bz-Nle-Lys-Arg-Arg-H. The virtual screening of docked analogs for favorable binding interactions along with synthetic feasibility directed us to a few molecules, which were then synthesized. Furthermore, the cytotoxic studies of these analogs followed by in vitro antiviral evaluation against NS2B-NS3 protease inhibition were performed.

Materials and methods

Materials

Substituted benzaldehyde, malonic acid, 4-aminoacetophenone, substituted o-phenylenediamine, acetic acid, phenylacetic acid, and thiol and chloroacetic acid were purchased from SD Fine Chem. Ltd., India. All other solvents used for synthesis were of LR grade. Quercetin was purchased from

Sigma Aldrich. The DENV2 serotype virus was obtained from patient serum samples. Madin–Darby canine kidney (MDCK) cells were obtained from National Centre for Disease Control, New Delhi, India.

Methods

Computational studies

Computational studies were carried out with the modeling package Discovery Studio v 3.1 (DS 3.1), Accelrys Inc., USA running on a Windows 7 platform. Docking studies were carried out with Genetic Optimization for Ligand Docking GOLD v 5.1.0 (CCDC, UK) running on a separate Red Hat Enterprise Linux WS Workstation.

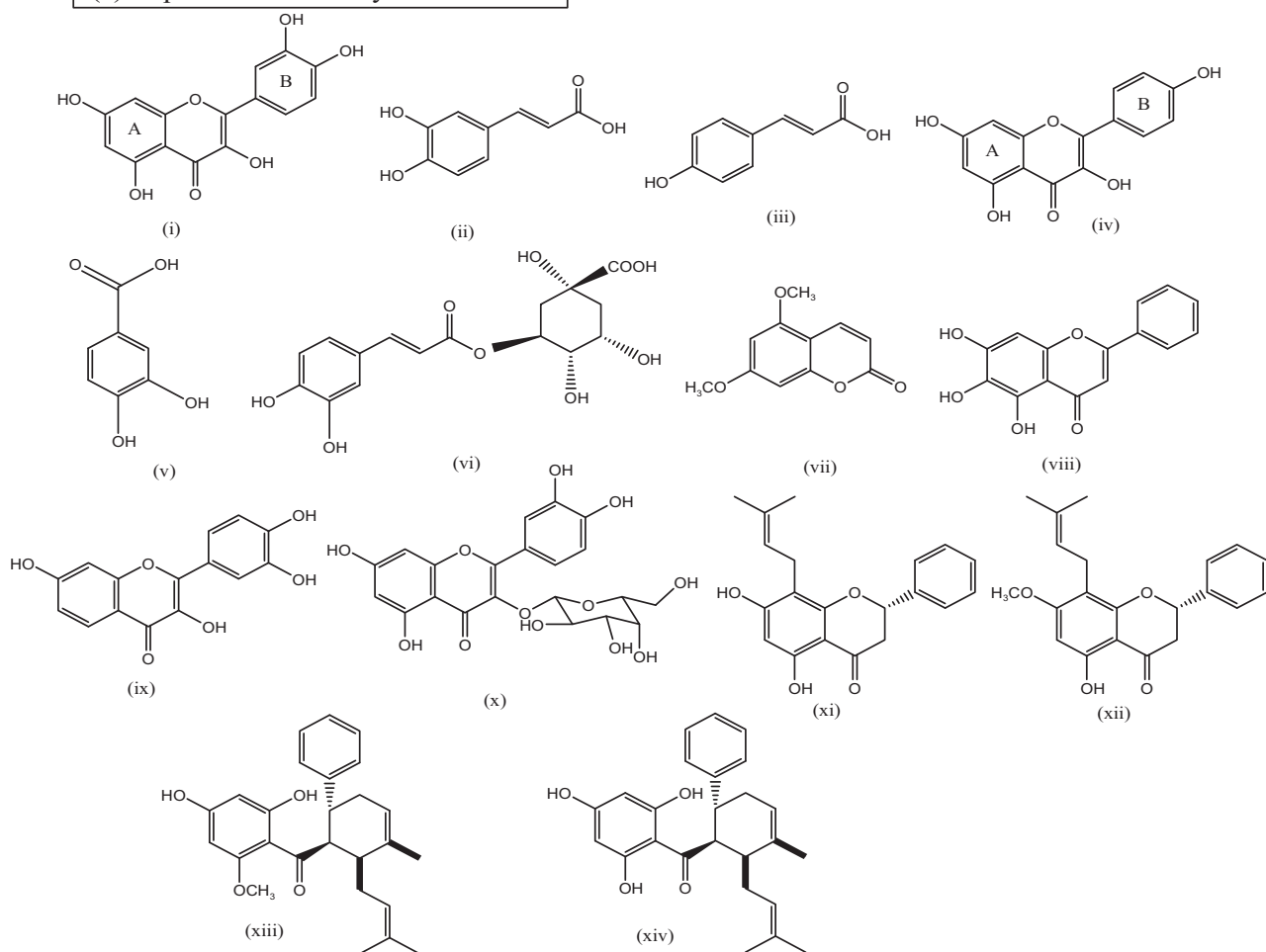
Preparation of enzyme and ligand for docking

The structure of available DENV2, which is a complex of NS2B-NS3 protease (PDB code: 2FOM), is devoid of any ligand. Thus, to get an insight into the binding cavity we used coordinates of co-crystallized ligand from West Nile virus (PDB code: 2FP7) belonging to the same family as that of DENV and that shares the structural similarity of the catalytic triad. It is available in complex with the inhibitor tetrapeptide Bz-Nle-Lys-Arg-Arg-H. The structure of DENV2 complexed with the inhibitor tetrapeptide Bz-Nle-Lys-Arg-Arg-H was constructed by homology modeling method described in Supplementary material.

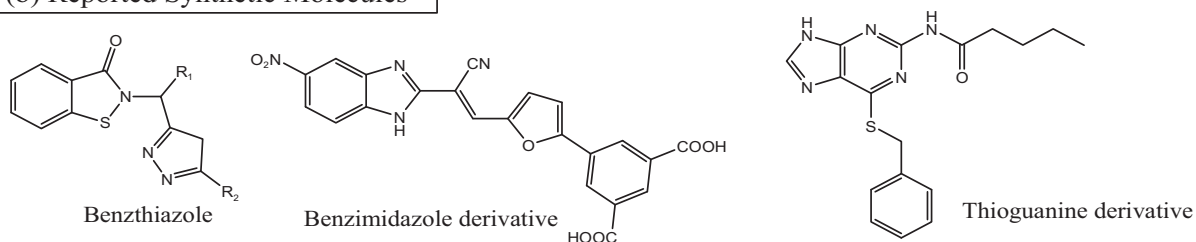
Preparation of enzyme and ligand for docking The protein complexed with ligand obtained from homology modeling was used for molecular docking studies. The enzyme was available in dimeric form; the monomeric unit of it was prepared and used for docking studies. Using CHARMM forcefield, the atom types and partial charges were defined and the hydrogen atoms were added at pH 8.5 to the monomeric unit and the formal charges for acidic and basic amino acids were defined accordingly. The prepared monomeric unit was then refined using CHARMM forcefield to a gradient of 0.1 kcal/mol/Å. Using the “Smart Minimizer” module of DS 3.1 with gradient of 0.01 kcal/mol/Å, the complexed ligand as well as the designed analogs were energy minimized. The validation of the docking protocol was done by redocking the complexed ligand, followed by superimposition of the crystal structure of ligand with the docked pose that showed RMSD 0.055.

Docking protocol GOLD software program was used to perform all calculations related to docking studies. This program uses a genetic algorithm (GA) for detecting the best-fit pose of ligand with respect to the protein, employing

(a) Reported Natural Phytoconstituents



(b) Reported Synthetic Molecules



(c) Designed target molecules scaffold

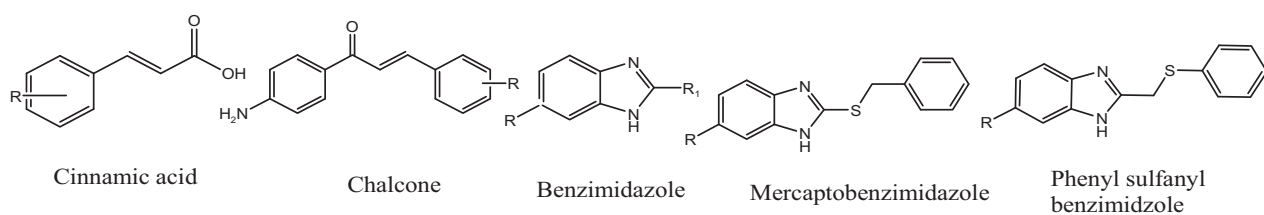


Fig. 1 Reported natural phytoconstituents (a) and reported synthetic molecules (b) along with structural features of the designed target molecules (c)

20 GA run iterations. While running the 20 GA runs for single structure, it uses a least-square routine as an attempt to form as many of the interactive hydrogen bonds as possible with the protein and the best fitted pose is assigned the fitness score. All the 20 GA runs generate 20 different poses of protein-ligand complex with the fitness score according to the quality of the solution and the best-fit analog is ranked with highest gold score. Similarly, all the designed analogs were studied using GOLD v 5.1.0, to explore the binding sites of these analogs within the targeted protein.

Synthesis The synthesis of designed analogs (Table 1) is described in the synthetic protocol. The purity of starting materials was assessed by determining their physical constant (*viz.* melting point) and by thin-layer chromatography (TLC) on Merck silica gel F_{254} plates. The progress of reactions was monitored by TLC. Physical constants were determined using the Analab melting point apparatus μ ThermoCal10 and the purity was analyzed by HPLC. The structures of the synthesized analogs were characterized by ^1H NMR and infrared spectroscopy (IR). NMR experiments were recorded on a 600-MHz Varian NMR spectrometer in dimethylsulfoxide (DMSO)- d_6 solvent, and data were processed by using Bruker Topspin 2.1 and Varian software. In proton NMR, 64 scans were recorded, chemical shifts have been reported in parts per million (ppm) using tetramethylsilane as an internal standard. IR experiments were recorded on Bruker Alpha-T spectrometer with 44 scans, and the data were processed using OPUS software.

Synthesis of cinnamic acid analogs (CA1–CA11)

The scheme (Scheme 1) is based on a Knoevenagel condensation reaction using substituted benzaldehyde (9 mmol) and dry malonic acid (24 mmol) in dry pyridine (20 ml) along with few drops of piperidine. The solution was heated at 80 °C on a water bath for 1 h. The reaction mixture was cooled and then acidified with HCl solution (~1.5–2 ml) to precipitate the product. Solid product was obtained, filtered, and recrystallized from ethanol.

Chemistry

3-phenyl prop-2-enoic acid (CA1) White crystals, yield (82%), m.p. 142 °C. IR (KBr) ν_{max} in cm^{-1} : 2825, 1671, 1448, 1311 (COOH), 1626, 1576 (C=C alkene), 1494 (Ar-C=C), 1175 (Ar-C-H); ^1H -NMR (DMSO- d_6 , 500 MHz) δ ppm 12.4 (s, 1H, COOH-1), 7.8 (d, 2H, H-2', H-6'), 7.69–7.68 (t, 2H, H-3', H-5'), 7.61–7.58 (d, 1H, H- β), 7.42–7.41 (t, 1H, H-4'), 6.55–6.52 (d, 1H, H- α). HPLC % purity = 99.81%.

3-(2-chlorophenyl) prop-2-enoic acid (CA2) White solid, yield (83%), m.p. 216–217 °C. IR (KBr) ν_{max} in cm^{-1} : 2518, 1681, 1417, 1304 (COOH), 1616, 1588 (C=C alkene), 1469 (Ar-C=C), 1222 (Ar-Cl), 1207 (Ar-C-H); ^1H -NMR (DMSO- d_6 , 500 MHz) δ ppm 12.65 (s, 1H, COOH-1), 7.93–7.92 (d, 1H, H-3'), 7.90–7.86 (d, 1H, H- β), 7.55–7.54 (d, 1H, H-6'), 7.46–7.43 (t, 1H, H-4'), 7.41–7.38 (t, 1H, H-5'), 6.63–6.59 (d, 1H, H- α). HPLC % purity = 99.82%.

3-(3-chlorophenyl) prop-2-enoic acid (CA3) White crystals, yield (89%), m.p. 148–150 °C. IR (KBr) ν_{max} in cm^{-1} : 2543, 1681, 1415, 1300 (COOH), 1636, 1595 (C=C alkene), 1573 (Ar-C=C), 1213 (Ar-Cl), 1138 (Ar-C-H); ^1H -NMR (DMSO- d_6 , 500 MHz) δ ppm 13.09 (s, 1H, COOH-1), 7.90–7.89 (d, 1H, H-4'), 7.80 (s, 1H, H-2'), 7.70–7.65 (t, 1H, H-5'), 7.59–7.55 (d, 1H, H- β), 7.44–7.41 (d, 1H, H-6'), 6.63–6.60 (d, 1H, H- α). HPLC % purity = 99.83%.

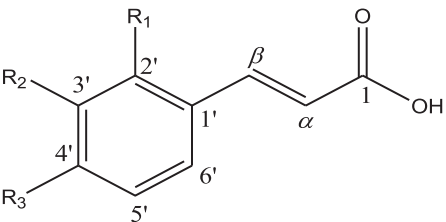
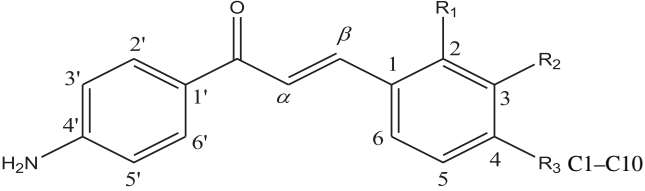
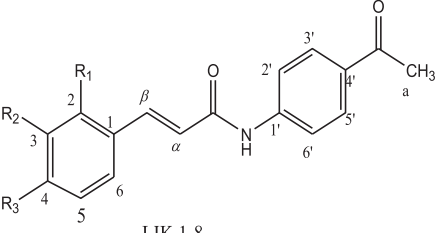
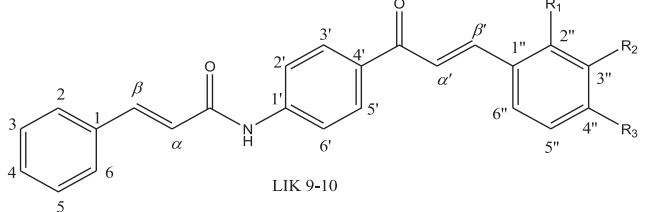
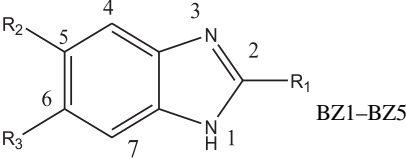
3-(4-chlorophenyl) prop-2-enoic acid (CA4) White crystalline solid, yield (95%), m.p. 255–256 °C. IR (KBr) ν_{max} in cm^{-1} : 2354, 1675, 1403, 1304 (COOH), 1623, 1589 (C=C alkene), 1568 (Ar-C=C), 1204 (Ar-Cl), 1175 (Ar-C-H); ^1H -NMR (DMSO- d_6 , 500 MHz) δ ppm 12.46 (s, 1H, COOH-1), 7.73–7.71 (d, 2H, H-3', H-5'), 7.60–7.57 (d, 1H, H- β), 7.47–7.42 (d, 2H, H-2', H-6'), 6.57–6.54 (d, 1H, H- α). HPLC % purity = 99.80%.

3-(2-methoxy-phenyl) prop-2-enoic acid (CA5) White solid, yield (91%), m.p. 192 °C. IR (KBr) ν_{max} in cm^{-1} : 1679, 1425, 1329 (COOH), 1618, 1489 (C=C alkene), 1462 (Ar-C=C), 1157, 1024 (C-O-C), 1102 (Ar-C-H); ^1H -NMR (DMSO- d_6 , 500 MHz) δ ppm 12.29 (s, 1H, COOH-1), 7.84–7.82 (d, 1H, H- β), 7.67–7.66 (d, 1H, H-6'), 7.41–7.39 (t, 1H, H-5'), 7.09–7.08 (d, 1H, H-3'), 6.99–6.97 (t, 1H, H-4'), 6.52–6.49 (d, 1H, H- α), 3.86 (s, 3H, OCH₃-2'). HPLC % purity = 99.79%.

3-(3-methoxy-phenyl) prop-2-enoic acid (CA6) White solid, yield (90%), m.p. 116–119 °C. IR (KBr) ν_{max} in cm^{-1} : 2966, 1666, 1421, 1315 (COOH), 1620, 1412 (C=C alkene), 1590 (Ar-C=C), 1167.9, 1109 (Ar-C-H), 1019.95 (C-O-C); ^1H -NMR (DMSO- d_6 , 500 MHz) δ ppm 12.35 (s, 1H, COOH-1), 7.54–7.52 (d, 1H, H-6'), 7.31–7.28 (d, s, 2H, H- β , H-2'), 7.23–7.21 (t, 1H, H-5'), 6.96–6.95 (d, 1H, H- α), 6.54–6.51 (d, 1H, H-4'), 3.76 (s, 3H, OCH₃-3'). HPLC % purity = 99.85%.

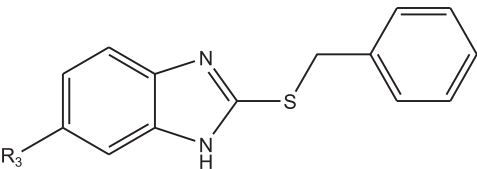
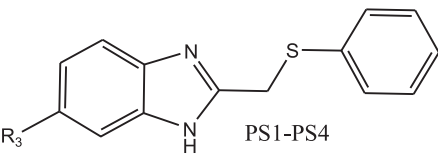
3-(4-methoxy-phenyl) prop-2-enoic acid (CA7) White solid, yield (95%), m.p. 179–180 °C. IR (KBr) ν_{max} in cm^{-1} : 2476, 1670, 1427, 1309 (COOH), 1621, 1510 (C=C alkene), 1596.95 (Ar-C=C), 1170 (Ar-C-H), 1025 (C-O-C); ^1H -NMR (DMSO- d_6 , 500 MHz) δ ppm 12.21 (s, 1H, COOH-1), 7.64–7.63 (d, 2H, H-2', H-6'), 7.56–7.53 (d,

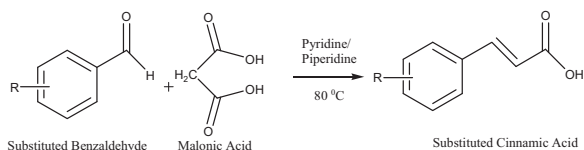
Table 1 Structure of all designed analogs with their codes

Scaffolds	Code	R ₁	R ₂	R ₃
 <p>CA1- CA11</p>	CA1	H	H	H
	CA2	Cl	H	H
	CA3	H	Cl	H
	CA4	H	H	Cl
	CA5	OCH ₃	H	H
	CA6	H	OCH ₃	H
	CA7	H	H	OCH ₃
	CA8	H	NO ₂	H
	CA9	H	H	NO ₂
	CA10	H	OH	H
	CA11	H	H	OH
 <p>C1-C10</p>	C1	H	H	H
	C2	Cl	H	H
	C3	H	H	Cl
	C4	OCH ₃	H	H
	C5	H	OCH ₃	H
	C6	H	H	OCH ₃
	C7	H	NO ₂	H
	C8	H	H	NO ₂
	C9	H	OH	H
	C10	H	H	OH
 <p>LIK 1-8</p>	LIK1	H	H	H
	LIK2	H	H	Cl
	LIK3	OCH ₃	H	H
	LIK4	H	H	OCH ₃
	LIK5	H	NO ₂	H
	LIK6	H	H	NO ₂
	LIK7	H	OH	H
	LIK8	H	H	OH
	LIK9	OCH ₃	H	H
	LIK10	H	OH	H
 <p>LIK 9-10</p>	BZ1	CH ₃	H	H
	BZ2	CH ₃	H	Cl
 <p>BZ1-BZ5</p>	BZ3	CH ₃	H	NO ₂
	BZ4	CH ₃	H	CH ₃
	BZ5	CH ₂ C ₆ H ₅	H	H

BZ1-BZ5

Table 1 (continued)

Scaffolds	Code	R ₁	R ₂	R ₃
 BS1-BS4	BS1	H	H	H
	BS2	H	H	Cl
	BS3	H	H	NO ₂
	BS4	H	H	CH ₃
 PS1-PS4	PS1	H	H	H
	PS2	H	H	Cl
	PS3	H	H	NO ₂
	PS4	H	H	CH ₃



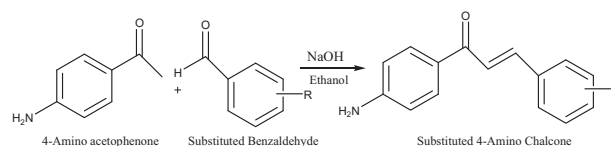
Scheme 1 Synthetic scheme for substituted cinnamic acid analogs

1H, H- β), 6.98–6.96 (d, 2H, H-3', H-5'), 6.39–6.36 (d, 1H, H- α), 3.799 (s, 3H, OCH₃- 4'). HPLC % purity = 98.88%.

3-(3-nitrophenyl) prop-2-enoic acid (CA8) Yellow crystals, yield (85%), m.p. 206–207 °C. IR (KBr) ν_{max} in cm⁻¹: 2523, 1684, 1420, 1301 (COOH), 1633, 1519 (C=C alkene), 1441 (Ar-C=C), 1357, 873 (NO₂), 1093 (Ar-C-H); ¹H-NMR (DMSO-d₆, 500 MHz) δ ppm 12.61 (s, 1H, COOH-1), 8.52 (s, 1H, H-2'), 8.25–8.23 (d, 1H, H-4'), 8.19–8.18 (d, 1H, H-6'), 7.75–7.69 (d, t, 2H, H- β , H-5'), 6.77–6.73 (d, 1H, H- α). HPLC % purity = 98.59%.

3-(4-nitrophenyl) prop-2-enoic acid (CA9) Yellow solid, yield (92%), m.p. 287 °C. IR (KBr) ν_{max} in cm⁻¹: 2513, 1683, 1425, 1225 (COOH), 1629, 1550 (C=C alkene), 1305, 868 (NO₂), 1225 (Ar-C=C), 1108 (Ar-C-H); ¹H-NMR (DMSO-d₆, 500 MHz) δ ppm 12.68 (s, 1H, COOH-1), 8.24 (d, 2H, H-3', H-5'), 7.98–7.97 (d, 2H, H-2', H-6'), 7.70–7.68 (d, 1H, H- β), 6.75–6.73 (d, 1H, H- α). HPLC % purity = 99.86%.

3-(3-hydroxy-phenyl) prop-2-enoic acid (CA10) Brown solid, yield (71.5%), m.p. 203 °C. IR (KBr) ν_{max} in cm⁻¹: 3377 (Ar-OH), 1668, 1450, 1332 (COOH), 1616, 1596 (C=C alkene), 1427 (Ar-C=C), 1178 (Ar-C-H); ¹H-NMR (DMSO-d₆, 500 MHz) δ ppm 12.35 (s, 1H, COOH-1), 9.58 (s, 1H, OH-3'), 7.50–7.48 (d, 1H, H- β), 7.23–7.20 (t, 1H, H-



Scheme 2 Synthetic scheme for substituted chalcone analogs

5'), 7.10–7.09 (d, 1H, H-6'), 7.008 (s, 1H, H-2'), 6.82–6.81 (d, 1H, H-4'), 6.41–6.39 (d, 1H, H- α). HPLC % purity = 99.82%.

3-(4-hydroxy-phenyl) prop-2-enoic acid (CA11) White solid, yield (50%), m.p. 208 °C. IR (KBr) ν_{max} in cm⁻¹: 3490 (Ar-OH), 2576, 1669, 1448, 1311 (COOH), 1626, 1589 (C=C alkene), 1511, 1421 (Ar-C=C), 1104 (Ar-C-H); ¹H-NMR (DMSO-d₆, 500 MHz) δ ppm 12.10 (s, 1H, COOH-1), 9.94 (s, 1H, OH-3'), 7.51–7.48 (d, 3H, H- β , H-2', H-6'), 6.80–6.78 (d, 1H, H- α), 6.29–6.27 (d, 2H, H-3', H-5'). HPLC % purity = 99.94%.

Synthesis of chalcone analogs (C1–C10)

The scheme (Scheme 2) is based on the Claisen–Schmidt condensation reaction to synthesize substituted chalcone. Equimolar quantities (7.1 mmol) of 4-aminoacetophenone and substituted benzaldehyde were dissolved in 30-ml absolute ethanol. Sodium hydroxide solution (20%, 5 ml) was added, and the resulting mixture was stirred at 10 °C for 2–4 h. The precipitate obtained was neutralized with HCl and then filtered and recrystallized from ethanol.

1-(4'-Amino-phenyl)-3-phenyl-prop-2-en-1-one (C1) Yellow crystals, yield (56%), m.p. 144 °C. IR (KBr) ν_{max} in cm⁻¹: 3350 (NH₂), 1650 (C=O), 1620, 1591 (C=C alkene),

1555, 1451 (Ar-C=C), 1131 (Ar-C-H); ¹H-NMR (DMSO-d₆, 500 MHz) δ ppm 7.94–7.93 (d, 2H, H-2', H-6'), 7.86–7.84 (d, t, 3H, H-2, H-6, H-4), 7.44 (d, t, d, 4H, H- α , H-3, H-5, H- β), 6.64–6.63 (d, 2H, H-3', H-5'), 6.17 (s, 2H, NH₂). HPLC % purity = 99.18%.

1-(4'-Amino-phenyl)-3-(2-chloro-phenyl)-prop-2en-1-one

(C2) Yellow solid, yield (78%), m.p. 106–109 °C. IR (KBr) ν_{max} in cm⁻¹: 3306, 3231 (NH₂), 1643 (C=O), 1608 (C=C), 1178 (Ar-Cl); ¹H-NMR (DMSO-d₆, 500 MHz) δ ppm 8.17–8.15 (d, 1H, H-6), 7.97–7.88 (m, 4H, H- β , J = 15.5 Hz, H-2', H-6', H- α , J = 15.5 Hz), 7.57–7.56 (d, 1H, H-3), 7.48–7.45 (m, 2H, H-4, H-5), 6.68–6.67 (d, 2H, H-3', H-5'), 6.17 (s, 2H, NH₂). HPLC % purity = 96.65%.

1-(4'-Amino-phenyl)-3-(4-chloro-phenyl)-prop-2en-1-one

(C3) Yellow solid, yield (80%), m.p. 157–159 °C. IR (KBr) ν_{max} in cm⁻¹: 3459, 3341 (NH₂), 1630 (C=O), 1602 (C=C), 1175 (Ar-Cl); ¹H-NMR (DMSO-d₆, 500 MHz) δ ppm 7.94–7.92 (d, 2H, H-2, H-6), 7.88–7.85 (m, 3H, H-2', H-6', H- β , J = 16 Hz), 7.62–7.59 (d, 1H, H- α , J = 16 Hz), 7.52–7.50 (d, 2H, H-3, H-5), 6.66–6.65 (d, 2H, H-3', H-5'), 6.08 (s, 2H, NH₂). HPLC % purity = 98.31%.

1-(4'-Amino-phenyl)-3-(2-methoxy-phenyl)-prop-2en-1-one

(C4) Yellow powder, yield (83%), m.p. 128 °C. IR (KBr) ν_{max} in cm⁻¹: 3335, 3217 (NH₂), 1243, 1022 (OCH₃), 1644 (C=O, α , β -unsaturated), 1593 (C=C alkene), 1521 (Ar-C=C), 1172 (Ar-C-H); ¹H-NMR (DMSO-d₆, 500 MHz) δ ppm 3.9 (s, OCH₃-2), 6.15 (s, NH₂-4'), 6.62–6.64 (d, H-3', H-5'), 7.01–7.04 (d, H- α , t, H-5), 7.10–7.12 (d, H-3), 7.41–7.44 (t, H-4), 7.80–7.83 (d, H- β), 7.90–7.94 (d, H-6, H-2', H-6'). HPLC % purity = 96.67%.

1-(4'-Amino-phenyl)-3-(3-methoxy-phenyl)-prop-2en-1-one

(C5) Brown powder, yield (75%), m.p. 145–146 °C. IR (KBr) ν_{max} in cm⁻¹: 3341, 3218 (NH₂), 1222, 1024 (OCH₃), 1649 (C=O, α , β -unsaturated), 1582 (C=C alkene), 1520 (Ar-C=C), 1171 (Ar-C-H); ¹H-NMR (DMSO-d₆, 500 MHz) δ ppm 3.85 (s, OCH₃-3), 6.06 (s, NH₂-4'), 6.66 (d, H-3', H-5'), 7.01 (d, H-4), 7.35–7.39 (t, H-5, d, H-6), 7.42 (s, H-2), 7.58–7.61 (d, H- α), 7.82–7.85 (d, H- β), 7.94 (d, H-2', H-6'). HPLC % purity = 99.36%.

1-(4'-Amino-phenyl)-3-(4-methoxy-phenyl)-prop-2en-1-one

(C6) Yellow solid, yield (88%), m.p. 108–111 °C. IR (KBr) ν_{max} in cm⁻¹: 3457, 3331 (NH₂), 1630 (C=O), 1599 (C=C), 1259, 1025 (C-O-C); ¹H-NMR (DMSO-d₆, 500 MHz) δ ppm 7.91–7.90 (d, 2H, H-2', H-6'), 7.79–7.78 (d, 2H, H-2, H-6), 7.72–7.69 (d, 1H, H- β , J = 15.5 Hz), 7.61–7.58 (d, 1H, H- α , J = 15.5 Hz), 7.02–7.01 (d, 2H, H-3, H-5), 6.65–6.64 (d, 2H, H-3', H-5'), 6.01 (s, 2H, NH₂), 3.86 (s, 3H, OCH₃). HPLC % purity = 97.55%.

1-(4'-Amino-phenyl)-3-(3-nitro-phenyl)-prop-2en-1-one

(C7) Orange solid, yield (68%), m.p. 165–168 °C. IR (KBr) ν_{max} in cm⁻¹: 3425, 3335 (NH₂), 1632 (C=O), 1609 (C=C), 1530, 1344 (NO₂); ¹H-NMR (DMSO-d₆, 500 MHz) δ ppm 8.69 (s, 1H, H-2), 8.30–8.29 (d, 1H, H-4), 8.25–8.23 (d, 1H, H-6), 8.07–8.04 (d, 1H, H- β , J = 16 Hz), 7.98–7.97 (d, 2H, H-2', H-6'), 7.76–7.71 (m, 2H, H-5, H- α , J = 16 Hz), 6.68–6.66 (d, 2H, H-3', H-5'), 6.17 (s, 2H, NH₂). HPLC % purity = 98.14%.

1-(4'-Amino-phenyl)-3-(4-nitro-phenyl)-prop-2en-1-one

(C8) Orange solid, yield (60%), m.p. 182–184 °C. IR (KBr) ν_{max} in cm⁻¹: 3459, 3338 (NH₂), 1646 (C=O), 1615 (C=C), 1545, 1344 (NO₂); ¹H-NMR (DMSO-d₆, 500 MHz) δ ppm 8.28–8.27 (d, 2H, H-3, H-5), 8.13–8.11 (d, 2H, H-2, H-6), 8.06–8.03 (d, 1H, H- β , J = 16 Hz), 7.97–7.95 (d, 2H, H-2', H-6'), 7.71–7.68 (d, 1H, H- α , J = 16 Hz), 6.67–6.66 (d, 2H, H-3', H-5'), 6.16 (s, 2H, NH₂). HPLC % purity = 98.99%.

1-(4'-Amino-phenyl)-3-(3-hydroxy-phenyl)-prop-2en-1-one

(C9) Yellow powder, yield (62%), m.p. 203–208 °C. IR (KBr) ν_{max} in cm⁻¹: 3343 (NH₂), 3231 (OH), 1644 (C=O), 1582, 1557 (C=C alkene), 1439 (Ar-C=C), 1132 (Ar-C-H); ¹H-NMR (DMSO-d₆, 500 MHz) δ ppm 9.58 (s, 1H, OH-3), 7.91–7.89 (d, 2H, H-2', H-6'), 7.76–7.73 (d, 1H, H- α), 7.53–7.50 (d, 1H, H- β), 7.26–7.21 (t, d, 2H, H-5, H-6), 7.17 (s, 1H, H-2), 6.84–6.83 (d, 1H, H-4), 6.63–6.61 (d, 2H, H-3', H-5'), 6.15 (s, 2H, NH₂). HPLC % purity = 92.28%.

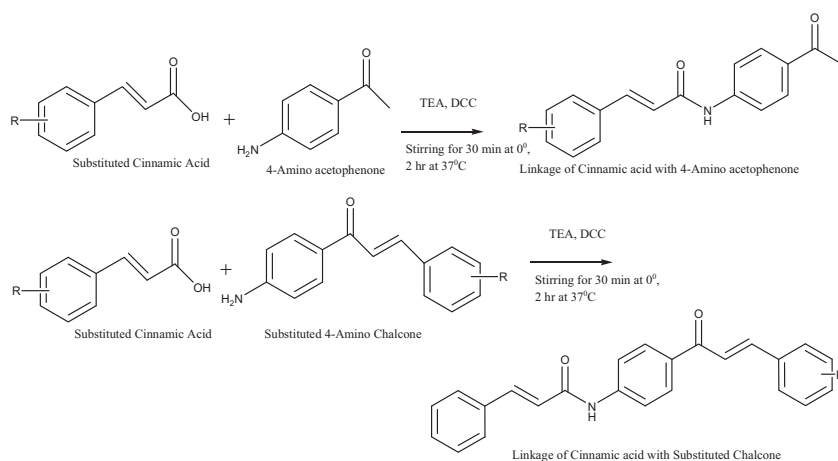
1-(4'-Amino-phenyl)-3-(4-hydroxy-phenyl)-prop-2en-1-one

(C10) Yellow powder, yield (58%), m.p. 173 °C. IR (KBr) ν_{max} in cm⁻¹: 3335 (NH₂), 3214 (OH), 1635 (C=O), 1625, 1588 (C=C alkene), 1507 (Ar-C=C), 1163 (Ar-C-H); ¹H-NMR (DMSO-d₆, 500 MHz) δ ppm 9.80 (s, 1H, OH-4), 8.20–8.19 (d, 2H, H-3, H-5), 7.91–7.90 (d, 1H, H- α), 7.57–7.54 (d, 2H, H-2', H-6'), 6.9–6.8 (d, 2H, H-2, H-6), 6.63–6.61 (d, 1H, H- β), 6.58–6.56 (d, 2H, H-3', H-5'), 6.2 (s, 2H, NH₂). HPLC % purity = 98.98%.

Synthesis of linkages of cinnamic acid (Lik1–Lik10)

Linkages of cinnamic acid with 4-aminoacetophenone and substituted 4-amino chalcone were synthesized as shown in Scheme 3. Cinnamic acid (10 mmol) was dissolved in 20 ml of dimethylformamide (DMF), followed by addition of triethanolamine (10 mmol). The solution was cooled in an ice bath, and 10 mmol of amine (4-aminoacetophenone or substituted 4-amino chalcone) was added. Then, a solution comprising of 10 mmol of N, N'-dicyclohexylcarbodiimide in 20 ml of dichloromethane was added in the reaction mixture. The mixture was stirred at 0 °C for 30 min and then

Scheme 3 Synthetic scheme for linkage of cinnamic acid with 4-aminoacetophenone (Lik1–Lik8) and 4-amino chalcone derivatives (Lik9–Lik10)



at 27 °C for 2 h. DMF was evaporated under reduced pressure, and the solution was diluted with 150 ml of water. The product was extracted with ethyl acetate; the extract was dried over sodium sulfate bed and evaporated. The residues were further recrystallized from methanol.

1-(4'-Acetyl-phenyl)-3-(phenyl)-prop-2-en-amide (Lik1)

White powder, yield (55%), m.p. 174–176 °C. IR (KBr) ν_{\max} in cm^{-1} : 3251.76, 763.76 (CO–NH), 2935.46, 2852.54, 1164.92, 1379.01 (CH_3), 1706.88 (C=O), 1645.17, 1541.02 (C=C alkene), 1596.95 (Ar–C=C), 3060.82 (Ar–C–H); $^1\text{H-NMR}$ (DMSO- d_6 , 500 MHz) δ ppm 3.05 (s, H-1), 6.32–6.35 (d, H-6), 7.00–7.03 (d, H-7), 7.24–7.25 (d, III-H, VI-H), 7.28–7.32 (t, IV-H, d, H-2', H-6'), 7.33 (d, II-H, VI-H), 7.43–7.45 (d, H-3', H-5'), 8.32 (s, NH-4). HPLC % purity = 99.96%.

1-(4'-Acetyl-phenyl)-3-(4-chloro-phenyl)-prop-2-en-amide (Lik2)

Buff powder, yield (78%), m.p. 220–221 °C. IR (KBr) ν_{\max} in cm^{-1} : 821.62 (Ar–Cl), 3325.05 (CO–NH), 2943.17, 2850.59, 1375 (CH_3), 1706.88 (C=O), 1623.95, 1537.16 (C=C alkene), 1569.95 (Ar–C=C), 1164.92 (Ar–C–H); $^1\text{H-NMR}$ (DMSO- d_6 , 500 MHz) δ ppm 2.2 (s, H-1), 5.58 (s, NH-4), 6.68–6.71 (d, H-5), 7.49–7.51 (d, H-III, H-V), 7.52–7.55 (d, H-6, H-II, H-VI), 7.61–7.63 (d, H-2', H-6'), 8.40–8.43 (d, H-3', H-5'). HPLC % purity = 94.54%.

1-(4'-Acetyl-phenyl)-3-(2-methoxy-phenyl)-prop-2-en-amide (Lik3)

Yellowish powder, yield (67%), m.p. 172 °C. IR (KBr) ν_{\max} in cm^{-1} : 1164.92, 1080.06 (Ar–OCH₃), 3253.69 (CO–NH), 2937.38, 2852.52, 891.05 (CH_3), 1704.96 (C=O), 1647.10, 1539.09 (C=C alkene), 1596.95 (Ar–C=C), 3060.80, 1228.57 (Ar–C–H); $^1\text{H-NMR}$ (DMSO- d_6 , 500 MHz) δ ppm 2.52 (s, H-1), 3.85 (s, OCH₃-II) 5.6 (s, NH-4), 6.64–6.67 (d, H-5), 6.77–6.80 (d, H-III), 6.99–7.00 (d, H-6), 7.07–7.11 (t, H-V), 7.48–7.51 (t,

H-IV, d, H-2', H-6'), 7.95–7.97 (d, H-VI), 8.40–8.42 (d, H-3', H-5'). HPLC % purity = 99.86%.

1-(4'-Acetyl-phenyl)-3-(4-methoxy-phenyl)-prop-2-en-amide (Lik4)

Yellowish white crystals, yield (72%), m.p. 190 °C. IR (KBr) ν_{\max} in cm^{-1} : 1382.87, 1170.71, 1027.99 (OCH₃), 3317.34, 779.19 (CO–NH), 2931.60, 2850.59, 1170.71 (CH_3), 1704.96 (C=O), 1645.17, 1510.16 (C=C alkene), 1602.74, 1544.88 (Ar–C=C), 3271.05, 1089.71 (Ar–C–H); $^1\text{H-NMR}$ (DMSO- d_6 , 500 MHz) δ ppm 2.5 (s, H-1), 3.80 (s, OCH₃-IV), 5.58 (s, NH-4), 6.47 (d, H-III, H-V), 6.98–6.99 (d, H-5), 7.34–7.37 (d, H-II, H-VI), 7.49–7.51 (d, H-6, d, H-2', H-6'), 7.88–7.90 (d, H-3', H-5').

1-(4'-Acetyl-phenyl)-3-(3-nitro-phenyl)-prop-2-en-amide (Lik5)

Yellowish white powder, yield (66%), m.p. 170 °C. IR (KBr) ν_{\max} in cm^{-1} : 1375.15, 736.76 (NO₂), 3294.19, 865.98 (CO–NH), 2933.53, 2856.38, 1352.01 (CH_3), 1701.10 (C=O), 1650.95, 1533.30 (C=C alkene), 1608.52 (Ar–C=C), 3082.04, 3041.53 (Ar–C–H); $^1\text{H-NMR}$ (DMSO- d_6 , 500 MHz) δ ppm 2.52 (s, H-1), 4.15 (s, NH-4), 6.86–6.89 (d, H-5), 7.66–7.69 (d, H-6), 7.71–7.74 (t, H-V), 8.06–8.08 (d, H-2', H-6', H-VI), 8.22–8.24 (d, H-3', H-5'), 8.42 (s, H-II), 8.46–8.48 (d, H-IV). HPLC % purity = 98.58%.

1-(4'-Acetyl-phenyl)-3-(3-hydroxy-phenyl)-prop-2-en-amide (Lik7)

White flakes, yield (65%), m.p. 227–229 °C. IR (KBr) ν_{\max} in cm^{-1} : 3328.91 (OH), 3267, 827.41 (CO–NH), 2929.67, 2850.59, 1166.85, 1309.58 (CH_3), 1782.10 (C=O), 1623.95 (C=C alkene), 1571.88 (Ar–C=C), 1087.78 (Ar–C–H); $^1\text{H-NMR}$ (DMSO- d_6 , 500 MHz) δ ppm 2.50 (s, H-1), 5.581 (s, NH-4), 6.84–6.86 (d, H-6, d, H-2', H-6'), 7.29–7.32 (t, H-V, d, H-IV), 7.67–7.69 (d, H-5, s, H-II), 8.43–8.44 (d, H-VI, H-3', H-5'), 10.16 (s, OH-III). HPLC % purity = 98.68%.

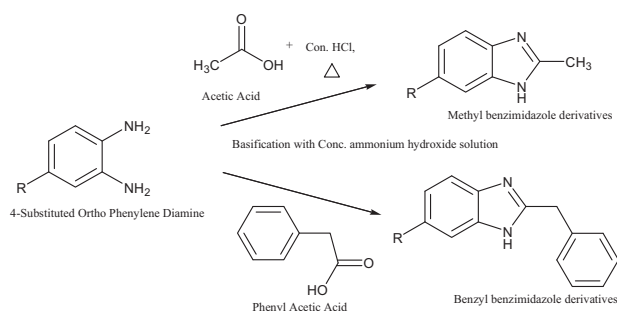
1-(4'-Acetyl-phenyl)-3-(4-hydroxy-phenyl)-prop-2-en-amide (Lik8) Yellowish white powder, yield (72%), m.p. 188–189 °C. IR (KBr) ν_{\max} in cm^{-1} : 3324 (OH), 2955, 892 (CO–NH), 2927, 2850, 1159 (CH_3), 1672 (C=O), 1626 (C=C alkene), 1574 (Ar–C=C), 1088 (Ar–C–H); $^1\text{H-NMR}$ (DMSO- d_6 , 500 MHz) δ ppm 2.48 (s, H-a), 6.54–6.57 (d, H α), 6.76–6.78 (d, H-3, H-5), 6.94–6.95 (d, H-2, H-6), 7.17–7.20 (d, H- β), 7.40–7.42 (d, H-2', H-6'), 8.390–8.403 (d, H-3', H-5'), 9.577 (s, OH-4), 5.552 (s, NH). HPLC % purity = 97.16%.

1-{4'-[3-(2''-methoxy-phenyl)-acryloyl]-phenyl}-3-phenyl-prop-2-en-amide (Lik9) White powder, yield (56%), m.p. 174–176 °C. IR (KBr) ν_{\max} in cm^{-1} : 3251.76, 763.76 (CO–NH), 2935.46, 2852.54, 1164.92, 1379.01 (CH_3), 1706.88 (C=O), 1645.17, 1541.02 (C=C alkene), 1596.95 (Ar–C=C), 3060.82 (Ar–C–H); $^1\text{H-NMR}$ (DMSO- d_6 , 500 MHz) δ ppm 8.32 (s, 1H, NH), 7.45–7.43 (d, 2H, H-2', H-6'), 7.33 (d, 2H, 2-H, 6-H), 7.32–7.28 (t, d, 3H, 4-H, H-3', H-5'), 7.25–7.24 (t, 2H, 3-H, 5-H), 7.03–7.00 (d, 1H, H- β), 6.35–6.32 (d, 1H, H- α), 3.05 (s, 1H, H-a). HPLC % purity = 96.24%.

1-{4'-[3-(3''-hydroxy-phenyl)-acryloyl]-phenyl}-3-phenyl-prop-2-en-amide (Lik10) Yellow crystals, yield (52%), m.p. 185–186 °C. IR (KBr) ν_{\max} in cm^{-1} : 2937.38, 2852.52, 1080.06 (Ar–OCH $_3$), 3253.69 (CO–NH), 1704.96 (C=O), 1647.10, 1539.09 (C=C alkene), 1596.95 (Ar–C=C), 3060.82 (Ar–C–H); $^1\text{H-NMR}$ (DMSO- d_6 , 500 MHz) δ ppm 8.42–8.40 (d, 2H, H-2, H-6), 7.97–7.95 (t, 3H, H-3, H-4, H-5), 7.51–7.48 (m, 4H, H-2', H-3', H-5', H-6'), 7.11–6.99 (m, 4H, H-3'', H-4'', H-5'', H-6''), 6.80–6.77 (d, 2H, H- β , H- β'), 6.67–6.64 (d, 2H, H- α , H- α'), 5.60 (s, 1H, NH), 3.81 (s, 3H, OCH $_3$). HPLC % purity = 88.76%.

Synthesis of substituted benzimidazole analogs (BZ1–BZ5)

Substituted o-phenylenediamine (20 mmol) and acetic acid or phenylacetic acid (30 mmol) were refluxed in presence of 20 cc 4-N HCl for 30–40 min (Scheme 4). The completion of the reaction is monitored by TLC, the reaction mixture



Scheme 4 Synthetic scheme for substituted benzimidazole analogs

was neutralized with ammonia hydroxide solution to precipitate the product, filtered and recrystallized from methanol.

2-Methyl-1H-benzimidazole (BZ1) Dark brown powder, yield (82%), m.p. 175 °C. IR (KBr) ν_{\max} in cm^{-1} : 3300 (NH), 1626 (C=N), 1420 (C–N), 2900 (Ar–C–H), 1504 (Ar–C=C), 3000 (CH_3); $^1\text{H-NMR}$ (DMSO- d_6 , 500 MHz) δ ppm 12.39 (s, NH-1), 3.34 (s, CH_3 -2), 6.51–6.55 (d, H-4), 7.42 (t, H-5), 7.68–7.69 (t, H-6), 7.58–7.61 (d, H-7). HPLC % purity = 98.47%.

4-Chloro-2-methyl-1H-benzimidazole (BZ2) Buff powder, yield (78%), m.p. 211–212 °C. IR (KBr) ν_{\max} in cm^{-1} : 3014 (NH), 1618 (C=N), 1456 (C–N), 2896 (Ar–C–H), 1545 (Ar–C=C), 803 (Ar–C–Cl); $^1\text{H-NMR}$ (DMSO- d_6 , 500 MHz) δ ppm 12.35 (s, NH-1), 2.45 (s, CH_3 -2), 7.09–7.10 (d, H-4), 7.41–7.42 (d, H-5), 7.47 (s, H-7). HPLC % purity = 98.07%.

4-Nitro-2-methyl-1H-benzimidazole (BZ3) Orange red powder, yield (72%), m.p. 227–229 °C. IR (KBr) ν_{\max} in cm^{-1} : 3436 (NH), 1624 (C=N), 1334, 1512 (NO_2); $^1\text{H-NMR}$ (DMSO- d_6 , 500 MHz) δ ppm 12.85 (s, NH-1), 2.54 (s, CH_3 -2), 7.59–7.61 (d, H-4), 8.02–8.04 (d, H-5), 8.33 (s, H-7). HPLC % purity = 99.75%.

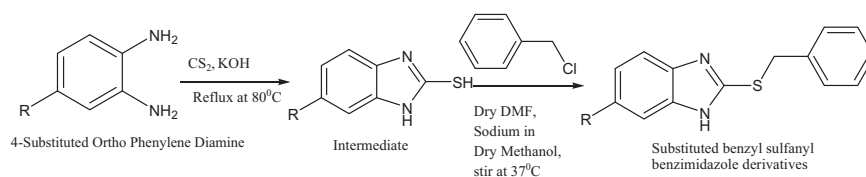
4-Methyl-2-methyl-1H-benzimidazole (BZ4) Blackish brown powder, yield (85%), m.p. 183–185 °C. IR (KBr) ν_{\max} in cm^{-1} : 3433.47 (NH), 1620.21 (C=N), 1440.04 (C–N), 3355.86 (Ar–C–H), 1497.72 (Ar–C=C), 2919.86, 2856 (Ar–C– CH_3); $^1\text{H-NMR}$ (DMSO- d_6 , 500 MHz) δ ppm 12.78 (s, NH-1), 2.62 (s, CH_3 -2), 2.43 (s, CH_3 -6), 7.05 (d, H-5), 7.38 (d, H-4), 8.17 (s, H-7). HPLC % purity = 97.97%.

2-Benzyl-1H-benzimidazole (BZ5) Dark brown shine powder, yield (63%), m.p. 191 °C. IR (KBr) ν_{\max} in cm^{-1} : 3048 (NH), 1587 (C=N), 1456 (C–N), 2732 (Ar–C–H), 1535 (Ar–C=C), 2835, 2922 (CH_3); $^1\text{H-NMR}$ (DMSO- d_6 , 500 MHz) δ ppm 12.37 (s, NH-1), 4.18 (s, CH_2), 7.47–7.48 (d, 4, 7-H), 7.29–7.30 (t, 5,6-H), 7.125–7.138 (m, 2', 6'-H, 3', 5'-H), 7.240 (t, 4'-H). HPLC % purity = 99.28%.

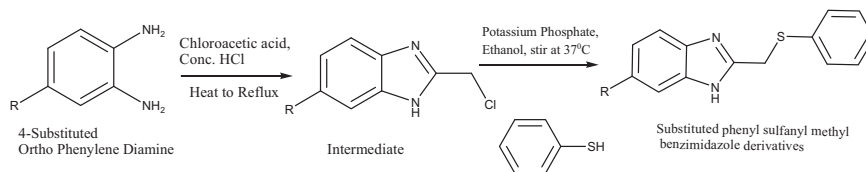
Synthesis of benzyl sulfanyl benzimidazole analogs (BS1–BS4)

Substituted o-phenylenediamine (19 mmol), carbon disulfide (22 mmol), and potassium hydroxide (22 mmol) in presence of ethanol and water were refluxed for 1 h (Scheme 5). After completion of the reaction, 20 ml of warm water and glacial acetic acid were added to precipitate the intermediate, recrystallized from methanol. To the

Scheme 5 Synthetic scheme for substituted benzyl sulfanylbenzimidazole analogs



Scheme 6 Synthetic scheme for substituted phenyl-sulfanyl methyl benzimidazole analogs



intermediate (15 mmol) in 25 ml of dry DMF, a solution of sodium (15 mmol) in dry methanol (7.5 ml) was added and stirred for 20 min at room temperature. To this, benzyl chloride (15 mmol) was added drop-wise, stirring was continued till the reaction completed. The final product was precipitated by pouring the reaction mixture into crushed ice water, filtered, and air-dried.

2-(Benzyl-sulfanyl)-1H-benzimidazole (BS1) Dark brown shine crystals, yield (58%), m.p. 192 °C. IR (KBr) ν_{max} in cm^{-1} : 3300 (NH), 1626 (C=N), 1415 (C-N), 3016 (Ar-C-H), 1524 (Ar-C=C), 2956, 2814 (CH₂), 706 (C-S); ¹H-NMR (DMSO-d₆, 500 MHz) δ ppm 12.549 (s, NH-1), 4.543 (s, CH₂), 7.413–7.425 (d, 4, 7, 2', 6'-H), 7.093–7.107 (t, 5, 6-H), 7.271–7.296 (t, 3', 5'-H), 7.211–7.235 (t, 4'-H). HPLC % purity = 94.99%.

2-(Benzyl-sulfanyl-6-chloro)-1H-benzimidazole (BS2) Brown shine crystals, yield (67%), m.p. 139–140 °C. IR (KBr) ν_{max} in cm^{-1} : 3321 (NH), 1622 (C=N), 1423 (C-N), 3045 (Ar-C-H), 1528 (Ar-C=C), 2961, 2853 (CH₂), 825 (C-Cl); ¹H-NMR (DMSO-d₆, 500 MHz) δ ppm 12.732 (s, NH-1), 4.542 (s, CH₂), 7.115–7.129 (d, 4-H), 7.410–7.422 (s, 2', 6'-H), 7.489 (s, 7-H), 7.273–7.298 (t, 3', 5'-H), 7.227–7.239 (t, 4'-H). HPLC % purity = 99.17%.

2-(Benzyl-sulfanyl-6-nitro)-1H-benzimidazole (BS3) Brown powder, yield (77%), m.p. 223–225 °C. IR (KBr) ν_{max} in cm^{-1} : 3584, 3326 (NH), 1628 (C=N), 1438 (C-N), 3103 (Ar-C-H), 1594 (Ar-C=C), 2924, 2818 (CH₂), 698 (C-S), 1517, 1316 (N-O); ¹H-NMR (DMSO-d₆, 500 MHz) δ ppm 2.534 (s, CH₂), 7.257–7.271 (d, H-3', H-5'), 7.613–7.599 (t, d, H-4', H-2', H-6'), 7.846 (s, H-4), 8.038–8.026 (d, H-5), 8.332 (s, H-7), 13.023 (s, NH). HPLC % purity = 95.92%.

2-(Benzyl-sulfanyl-6-methyl)-1H-benzimidazole (BS4) Dark brown powder, yield (75%), m.p. 232–234 °C. IR (KBr) ν_{max} in cm^{-1} : 3033.20 (NH), 1625.61 (C=N), 1425.63 (C-N), 1520.94 (Ar-C=C), 2715.74 (CH₂), 2970.17, 2762.89 (CH₃), 693.35 (C-S), 2604.37 (C-H); ¹H-

NMR (DMSO-d₆, 500 MHz) δ ppm 2.6 (s, CH₃-6), 2.7 (s, CH₃-4'), 4.3 (s, CH₂), 7–7.6 (m, H-4', H-2', H-6', H-4, H-5, H-7). HPLC % purity = 98.32%.

Synthesis of phenyl-sulfanyl methyl benzimidazole analogs (PS1–PS4)

Substituted o-phenylenediamine (26 mmol), chloroacetic acid (20.8 mmol), and hydrochloric acid 5 ml were refluxed until the reaction completed (Scheme 6). The reaction mixture was poured in water and basified using an ammonium hydroxide solution to precipitate the intermediate. An equimolar quantity of intermediate, thiol in presence of potassium phosphate, and ethanol were stirred at room temperature until reaction completed that was observed by TLC. The reaction mixture was diluted with water and extracted with ethyl acetate. The organic layer was dried on anhydrous sodium sulfate and removed in a vacuum.

2-(Phenyl-sulfanyl-methyl)-1H-benzimidazole (PS1) Dark brown powder, yield (51%), m.p. 282 °C. IR (KBr) ν_{max} in cm^{-1} : 3382 (NH), 1625 (C=N), 1455 (C-N), 3056 (Ar-C-H), 1533 (Ar-C=C), 2964, 2853 (CH₂), 736 (C-S); ¹H-NMR (DMSO-d₆, 500 MHz) δ ppm 12.513 (s, NH-1), 4.428 (s, CH₂), 7.169 (d, 4, 7-H), 7.120–7.129 (t, 5, 6-H), 7.383–7.396 (d, 1', 6'-H), 7.465–7.473 (t, 3', 5'-H), 7.264–7.289 (t, 4'-H). HPLC % purity = 99.50%.

2-(Phenyl-sulfanyl-methyl-6-chloro)-1H-benzimidazole (PS2) Buff powder, yield (58%), m.p. 155 °C. IR (KBr) ν_{max} in cm^{-1} : 3388 (NH), 1621 (C=N), 1468 (C-N), 3098 (Ar-C-H), 1582 (Ar-C=C), 2928, 2854 (CH₂), 702 (C-S), 807 (C-Cl); ¹H-NMR (DMSO-d₆, 500 MHz) δ ppm 12.23 (s, NH-1), 4.25 (s, CH₂), 7.51–7.52 (d, 4-H), 7.21–7.24 (s, 2', 6'-H), 7.32 (s, 7-H), 7.15–7.16 (t, 3', 5'-H), 7.28–7.32 (t, 4'-H). HPLC % purity = 99.62%.

2-(Phenyl-sulfanyl-methyl-6-nitro)-1H-benzimidazole (PS3) Light brown powder, yield (54%), m.p. 196 °C. IR (KBr) ν_{max} in cm^{-1} : 3567 (NH), 1629 (C=N), 1451

(C–N), 3110 (Ar–C–H), 1593 (Ar–C=C), 2923, 2852 (CH₂), 733 (C–S), 1515, 1341 (N–O); ¹H-NMR (DMSO-d₆, 500 MHz) δ ppm 12.883 (s, NH-1), 4.499 (s, CH₂), 7.493–7.506 (d, 4-H), 7.603 (d, 5-H), 8.336 (s, 7-H), 8.026–8.040 (d, 2', 6'-H), 7.352–7.377 (t, 3', 5'-H), 7.260–7.285 (t, 4'-H).

2-(Phenyl-sulfanyl-methyl-6-methyl)-1H-benzimidazole

(PS4) Brown powder, yield (62%), m.p. 252–254 °C. IR (KBr) ν_{max} in cm⁻¹: 3035.37 (NH), 1622.85 (C=N), 1445.57 (C–N), 1586.58 (Ar–C=C), 2858.71 (CH₂), 2918.35 (CH₃), 739.45 (C–S); ¹H-NMR (DMSO-d₆, 500 MHz) δ ppm 2.4 (s, CH₃), 9.6 (s, NH-1), 4.6 (s, CH₂), 7–7.4 (m, 3', 5'-H, 4'-H, 7-H), 7.6 (d, 5-H), 7.8 (d, 2', 6'-H). HPLC % purity = 93.24%.

Cytotoxicity studies

MTT-Formazan assay (3-(4, 5-dimethylthiazol-2-yl)-3, 5-diphenyl tetrazolium bromide) was used to determine the cytotoxicity of all synthesized analogs [11]. MDCK cells were grown in 96-well plates for 24 h till 85–90% confluency. After 24 h, the media of serially diluted compounds (tenfold dilution) was added to replace the plates. After 16 h of incubation, the medium was removed and 100- μ L MTT solution was added to each well and incubated at 37 °C for 4 h. The supernatant layer was removed followed by addition of 100 μ L of DMSO to dissolve formazan crystals. Absorbance was measured at 540 nm in a microplate reader. The equation used to normalize the data is:

$$\text{Cell viability}(\%) = \frac{(\text{Sample value} - \text{blank control})}{(\text{Cell control} - \text{blank control})} \times 100.$$

A dose–response curve was plotted via nonlinear regression (curve fit). The cytotoxic concentration i.e., CC₅₀ was defined as the concentration required to reduce cell viability by 50%.

Expression and purification of DENV2 NS2B-NS3 protease

DENV2 NS2B-NS3 plasmid construct was cloned in pRSET Vector A. The cloned plasmid was transformed in to *Escherichia coli* B121(DE3) cells and grown in Luria Bertani media containing ampicillin (100 μ g/ml) at 37 °C with continuous shaking until the OD₆₀₀ reached to 0.6. Expression was induced by 0.6-mM IPTG, and cells were further grown for 18 h at 18 °C. The cells were pelleted at 8000 rpm for 10 min and resuspended in lysis buffer (100-mM Tris, pH 8.0, 150-mM NaCl, 10-mM imidazole, and 5% glycerol). The cells were lysed on ice by sonication using ultrasonic processor. The lysate was subjected to centrifugation at 10000 rpm for 45 min and supernatant was

separated. The purification was performed using Ni-NTA column chromatography. The Ni-NTA agarose resin was pre-equilibrated with binding buffer and the supernatant was incubated with resin for 2–3 h at 4 °C. The supernatant was passed through column and washed with lysis buffer containing 20–50-mM imidazole. The protein was eluted in lysis buffer containing 250-mM imidazole. The protein fractions were pooled and dialyzed at 4 °C using 10-kDa cutoff membrane against dialysis buffer (100-mM Tris, pH 8.0, 150-mM NaCl, and 5% glycerol). Protein concentration was determined by the Bradford assay using BSA as a standard, and the aliquots were stored at –80 °C in 25% glycerol [1].

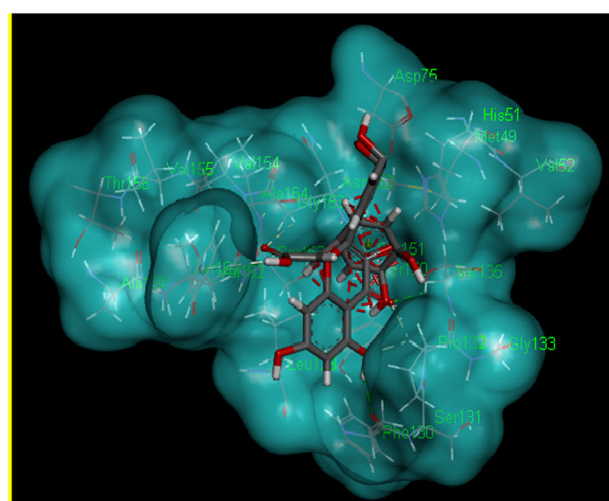
DENV2 NS2B-NS3 protease inhibition assay

The enzymatic inhibition was assayed using a fluorogenic substrate, Bz-Nle-Lys-Arg-Arg-AMC (Bachem) in a 96-well plate. Briefly, 50 μ L of reaction containing purified NS2B-NS3 protease in assay buffer (100-mM Tris–HCl pH 9, 1-mM CHAPS and 20% glycerol) with different dilutions of the analogs (10–500 μ M) was pre-incubated for 15 min at 37 °C. Finally, 20 μ M of substrate was added to the reaction mixture and incubated at 37 °C for 1 h. The substrate hydrolysis was monitored as relative fluorescence units (RFUs) at an excitation and emission wavelengths of 380 and 460 nm, respectively, in a multimode microplate reader (Bio-Rad). The assay was performed twice in duplicates, and IC₅₀ values were calculated using nonlinear regression models in Graph Pad Prism 5.01 software. Prior to the inhibitory assays, protease assay without analogs was performed to monitor the activity of NS2B-NS3. Protease activity was measured as the increase in RFUs. Quercetin was used as a reference compound.

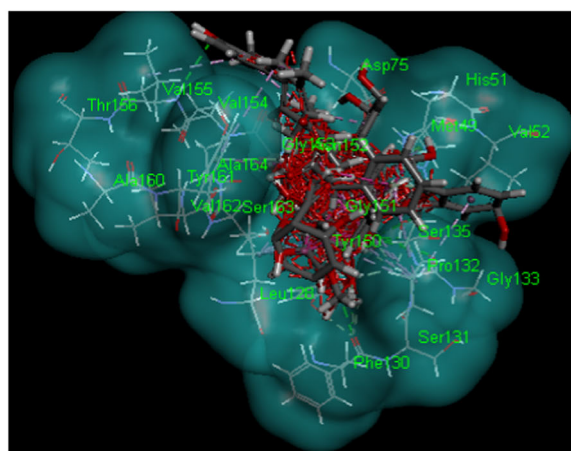
Result and discussion

Molecular docking

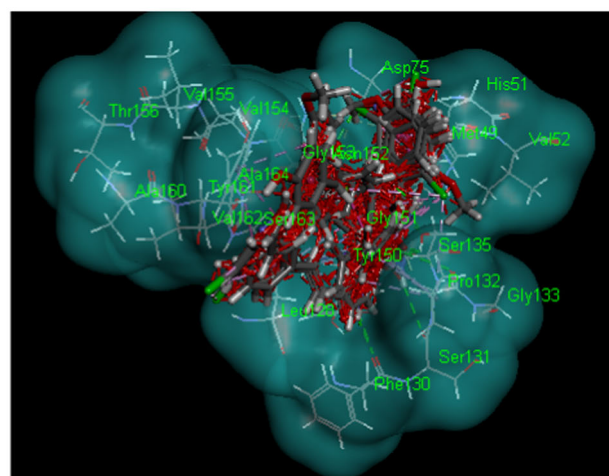
In NS2B-NS3 protease complex of DENV, the NS3 protein consists of the catalytic triad of Ser135-His51-Asp75. These catalytic residues take a form of an oxyanion stabilized by hydrogen bond formed between the hydroxyl group of serine with imidazole nitrogen of histidine, which in turn is hydrogen-bonded to the aspartic carboxyl group [9]. The catalytic mechanism known to be involved is nucleophilic attack of the oxygen atom in serine hydroxyl group, which in turn results into the cleavage of electrophilic carbon in the peptide bond. Consequently, a tetrahedral intermediate is formed, and this is stabilized by hydrogen bonds involving Gly151, Gly153, and Tyr161. Hence, it is believed that any molecule, which can interact with these residues, can



(a)



(b)



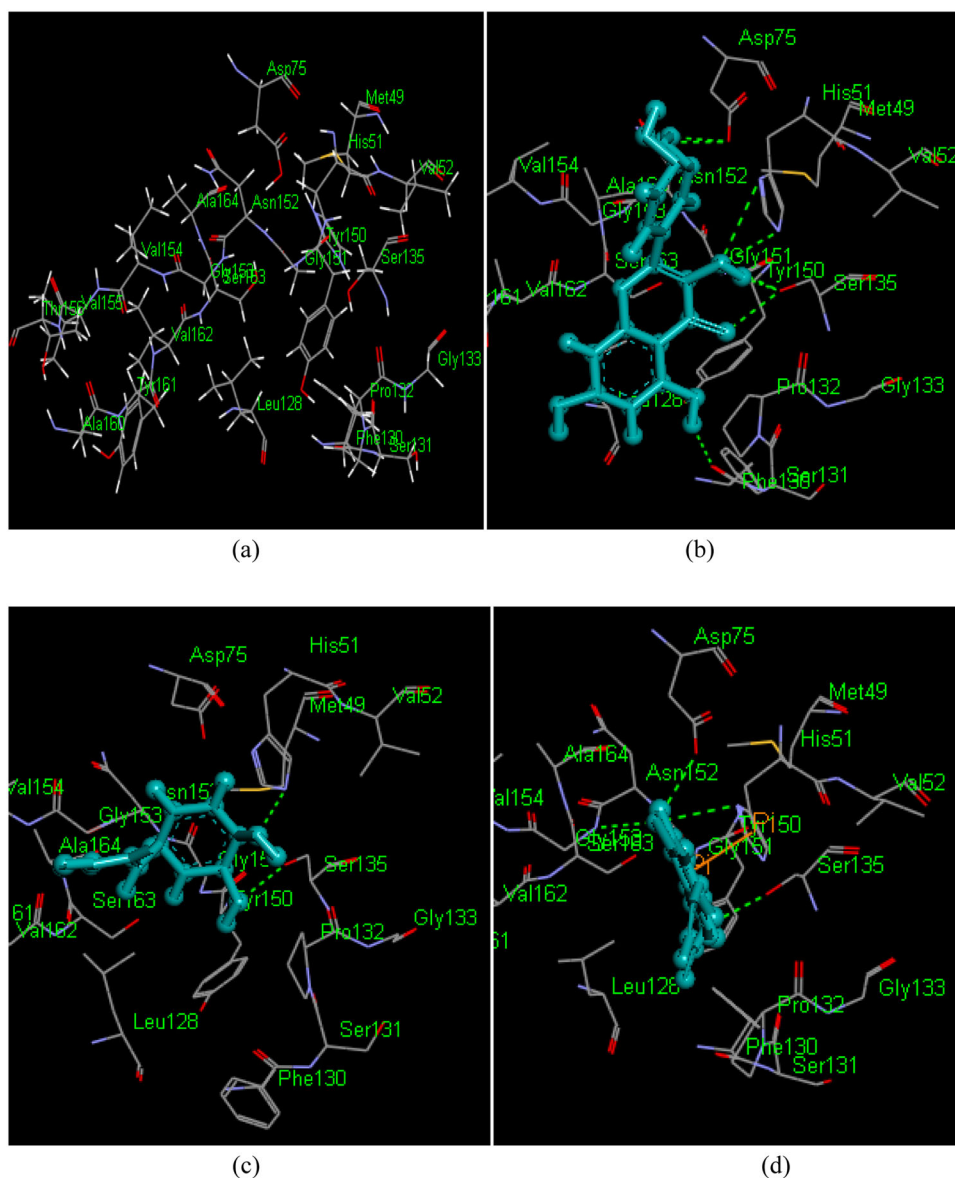
(c)

Fig. 2 Docked poses of quercetin and caffeic acid (a) and all the natural phytoconstituents occupying and interacting with the catalytic triad (His51-Asp75-Ser135) of NS2B-NS3 protease of DENV (b), and all the designed analogs occupying the catalytic triad of NS2B-NS3 protease of DENV (c)

inhibit the function of DENV protease. We have docked the reported natural phytoconstituents showing anti-dengue activity, along with our designed analogs in the reconstructed protein 2FOM considering quercetin as standard. It was observed that quercetin showed interactions with all the catalytic triad residues via hydrogen bonding, which is in the agreement with its reported activity against DENV. The hydroxyl group of the B-ring of quercetin interacted with Asp75 whereas hydroxyl group at A-ring interacted with Phe130. The hydroxyl group of pyrone ring interacted with His51 and Ser135, while carbonyl group of the pyrone ring interacted with Ser135. In case of other phytoconstituents caffeic acid, protocatechic acid, and coumarin, they showed interactions with two of the catalytic triad residues along with other residues such as Tyr150, Gly151, and Gly153. Whereas p-coumeric acid, showed no interaction with catalytic triad but interacted with Gly151, that is known as the important residue in stabilizing the tetrahedral intermediate. Baicalein showed hydrophobic interaction with His51 and remaining phytoconstituents did not interact with triad residues but showed interactions with other important residues Tyr150, Gly151, and Gly153. The docking interactions of natural phytoconstituents are shown in Supplementary material (Supplementary Table S1).

Depending on the molecular interaction results of phytoconstituents with the catalytic triad, different scaffolds were designed. Cinnamic acid analogs (CA1–CA11) were designed based on caffeic acid and p-coumaric acid scaffolds. Similarly, chalcone series (C1–C10) was designed based on quercetin scaffold, which is a flavone, a cyclized form of hydroxychalcone. The molecular hybrid approach was used to link caffeic acid and chalcone (Lik1–Lik10), both of the scaffolds being antivirals. Many synthetic molecules based on benzimidazole scaffold are also reported as well as patented for their antiviral activity [12]. Based on these observations, different benzimidazole analogs were designed (BZ1–BZ5, BS1–BS4, and PS1–PS4). We have docked our designed analogs in NS2B-NS3 protease to get insight of their binding interactions with the above important residues (Supplementary Table S2). It was observed that most of the designed analogs showed similar pattern of interactions comparable to the phytoconstituents discussed above. In cinnamic acid analogs, the acidic carbonyl group interacted with carboxylic hydrogen of Ser135 while the substituents (such as chloro, methoxy, nitro, and hydroxyl) showed interaction with Asp75. The aromatic ring had the hydrophobic interaction with His51. In chalcone analogs, the free amino group interacted with Ser135. Apart from triad residue they were observed to interact with other residues such as Gly151, Gly153, Tyr161, Tyr150, Phe150, Pro132, and Ser131. In case of

Fig. 3 Detailed view of catalytic triad (a) and molecular interactions of quercetin (b), caffeic acid (c), and designed analog CA2 (d)

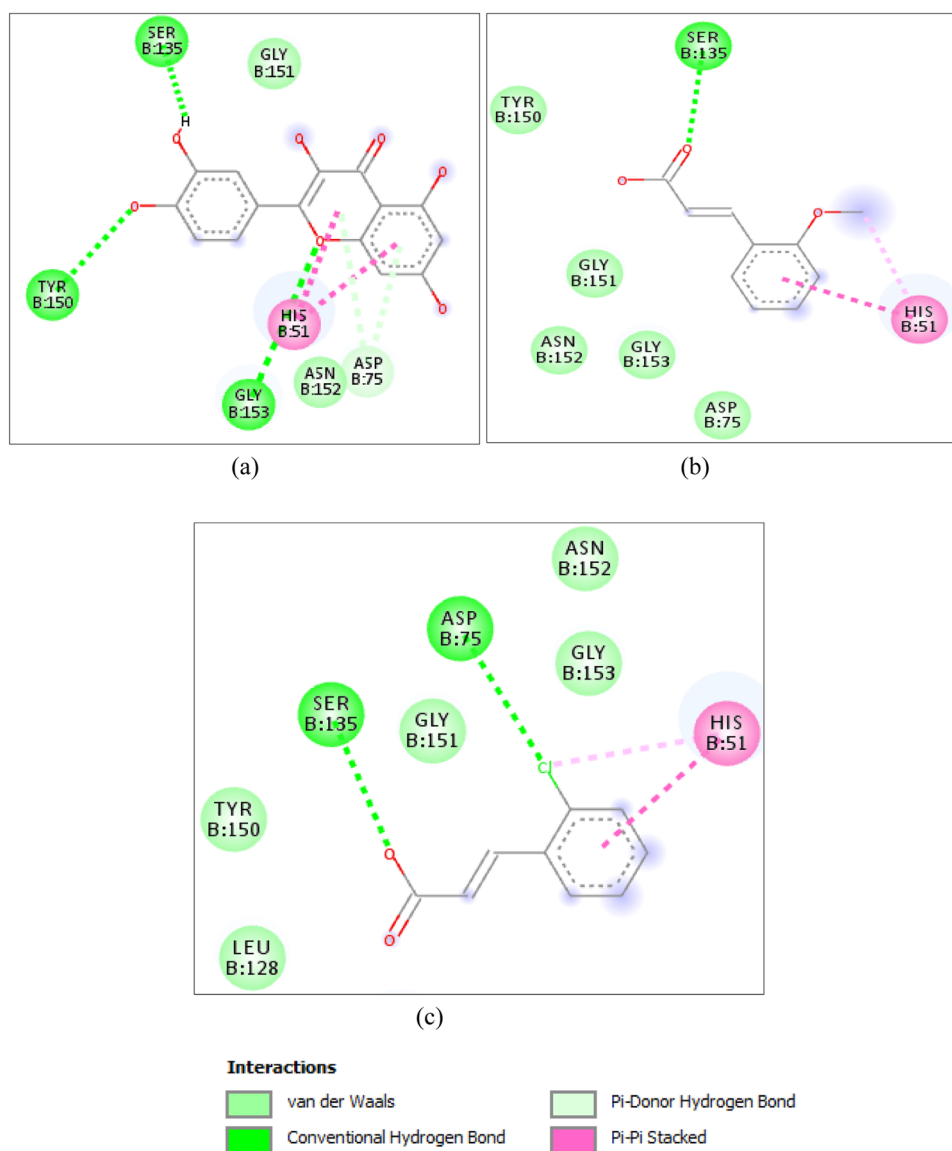


linkage of cinnamic acid, the amide bond interacted with Ser135, Tyr150, and the aromatic ring had the hydrophobic interaction with His51. In benzimidazole, benzyl sulfanyl benzimidazole, and phenyl sulfanyl benzimidazole analogs, the heteroatom in the ring showed interactions with Tyr150 and Phe130 while the aromatic ring showed hydrophobic interaction with His51. The substituted functional groups on the aromatic ring of all the above-mentioned rings interacted mainly with Ser135. The above observations indicated that the designed analogs of different scaffolds showed interactions with the catalytic triad as well as other important residues. This might lead to the inhibition of NS2B-NS3 protease of DENV. The docking interactions of phytoconstituents and designed analogs are shown in Figs. 2 and 3 and their 2D diagrams are shown in Fig. 4.

Synthesis

The computational studies of 14 natural phytoconstituents showed interactions with DENV protease residues. Based on molecular docking results, we have synthesized 44 analogs of different scaffolds viz. eleven cinnamic acid analogs (CA1–CA11), ten chalcone analogs (C1–C10), ten molecular hybrids of cinnamic acid and chalcone (Lik1–Lik10), and different other scaffolds based on benzimidazole (BZ1–BZ5, BS1–BS4, and PS1–PS4). The structures of all the synthesized molecules were confirmed after structural characterization by spectral technique such as IR and ^1H NMR spectroscopy. The IR spectra had shown the respective absorption bands for different functional groups, along with differentiating bands for aliphatic alkenes and aromatic double bonds. ^1H NMR spectra,

Fig. 4 2D representation of molecular interactions: quercetin (a), caffeic acid (b), and CA2 (c)



further confirmed the structure, based on the predictable delta values by protons of aromatic and aliphatic carbons of analogs.

Anti-dengue activity

Cytotoxicity studies

All the synthesized analogs were tested for cytotoxicity using the MTT-Formazan assay [11]. The concentration of analogs causing 50% reduction in cell viability (CC_{50}) was measured. The outcome of this study indicated that the synthesized analogs had no serious effect on MDCK cells (CC_{50} values are shown in Supplementary Table S3). Further, the anti-dengue activity of these nontoxic analogs was evaluated using the NS2B-NS3 protease inhibition assay.

NS2B-NS3 protease Inhibition

The in vitro protease inhibition assay was carried out as a quantitative evaluation to identify the inhibitory effect of our synthesized analogs. It is based on the measurement of fluorescence reflected by the cleavage of substrate due to the enzymatic activity of protease. Throughout the assay, protease enzyme concentration and the substrate concentration were maintained at 50-nM and 20 μ M, respectively. The inhibitory activity was measured by recording the fluorescence as RFU and every concentration was recorded in duplicate. It was compared with quercetin as standard drug by observing its effect at different concentration levels i.e., 10, 30, 50, 100, and 500 μ M. The synthesized analogs at different concentrations between 10 and 500 μ M were also measured in similar way. Experimentally used concentrations and measured RFU values

Table 2 Result of molecular testing against NS2B-NS3 protease inhibition assay

Sr. no.	Compound code	IC ₅₀ (μM)
	Std quercetin	28.73
1	CA1	35.07
2	CA2	27.33
3	CA7	57.68
4	CA11	217.8
5	C4*	113.3
6	C8	97.52
7	C9	47.91
8	C10	73.36
9	BZ1	25.84
10	BZ3	43.45
11	BS2	22.19
12	BS3	136.2
13	PS2	42.77

* $p = 0.3457$

were used to determine the inhibitory concentration (IC₅₀) of the individual drug. The standard quercetin IC₅₀ value was 28.73 μM, in case of cinnamic acid analogs CA2 was showing the lower IC₅₀ value than the standard 27.33 μM whereas CA1 and CA7 were showing the comparable IC₅₀ value to that of the standard 35.07 and 57.68 μM, respectively. In chalcone analogs, C9 was showing the comparable IC₅₀ value with 47.91 μM, C10 and C9 were shown IC₅₀ values of 73.36 and 97.52 μM. In case of benzimidazole analogs, BZ1 and BS2 were showing the lower IC₅₀ value than the standard 25.84 and 22.19 μM, respectively, and BZ4 and PS2 showing the IC₅₀ values of 43.45 and 42.77 μM, respectively. The evaluated IC₅₀ values are shown in Table 2, and Fig. 5 shows the nonlinear regression curve fit representation. The analogs whose IC₅₀ values were lower and comparable with standard with the r^2 above 0.9 were considered for further discussion. The recorded fluorescence reading in duplicate as RFU and biological replicates ($n \geq 2$) was considered for analysis. For assays, $p < 0.05$ (Mann–Whitney U test and Student's t test) was considered statistically significant and the analogs showing $p > 0.3$ shown in the Table 2 by indicating with * mark.

The designed analogs were developed based on the important structural features of reported natural phytoconstituents, and the activity results were in agreement with the observations. Although, the scaffolds tend to exhibit varied degree of NS2B-NS3 protease inhibition but some similar pattern of interactions was observed with respect to the scaffolds. For e.g., in case of cinnamic acid analogs, the free carboxyl group was interacting with the catalytic triad along with the other crucial amino-acid residues. In chalcone analogs, the free amino

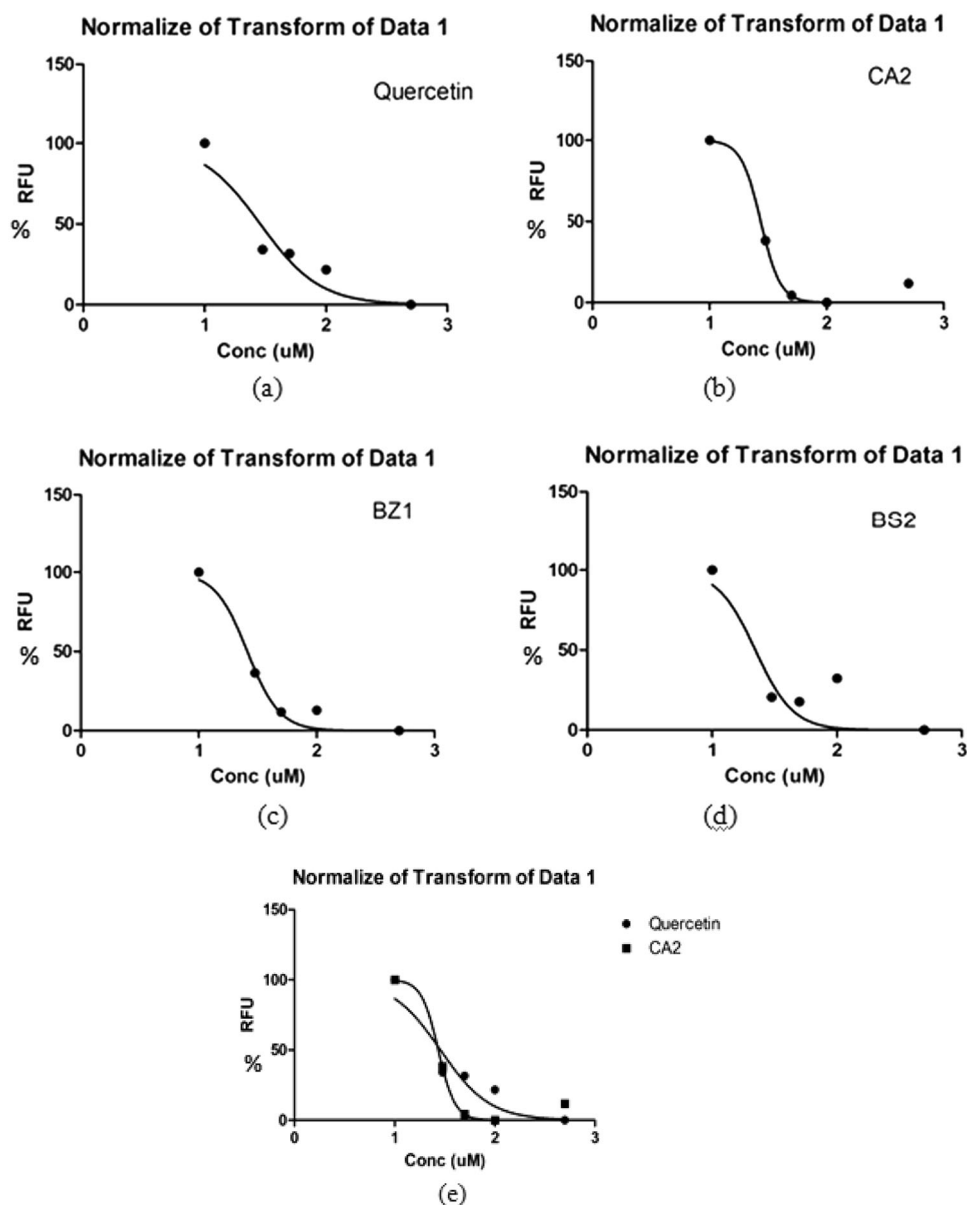
group was observed to form the hydrogen bond with the catalytic as well as the important amino-acid residues. Moreover, the aromatic ring of all designed analogs showed the hydrophobic interaction with triad residue as expected and, it was observed that incorporating more than three hydrophobic rings did not show additive effect. Analogues with various substituents such as electron-withdrawing, electron-donating were considered. Substitution of chloro, methyl, and methoxy functional groups at ortho and meta position was observed to have additive effect for protease inhibition.

Two analogs from benzimidazole scaffold (BS2 and BZ1) and one from cinnamic acid scaffold (CA2) showed more potent protease inhibition compared to standard quercetin, while CA1 showed comparable potency, which was in agreement with the docking results. The comprehensive examination revealed that two chloro substituted analogs (BS2 and CA2) and two unsubstituted analogs (BZ1 and CA1) showed more potency than the standard quercetin. The docking results indicated that CA2 interacted with all the amino acids in the catalytic triad by forming direct hydrogen bond. The free carboxyl group showed interaction with Ser135, chloro group showed hydrogen bond with Asp75 and Gly153, whereas the aromatic ring showed hydrophobic interaction with His51 (π - π). Similar pattern of interactions was observed with the standard. In case of unsubstituted cinnamic acid (CA1), the free carboxyl group interacted with Ser135. Similar pattern of interactions was observed in case of benzimidazole scaffold too. The other analogs, which showed comparable inhibitory activity to that of standard, had different substituents like methyl, methoxy, hydroxyl, and nitro groups (PS2, BZ4, C9, CA7, C10, and C8) but all these interacted similarly with the catalytic triad by forming the hydrogen bond with the Ser135. Along with Ser135, some also interacted with Tyr161 and Gly151.

Other analogs, which interacted with the catalytic triad residues and having IC₅₀ value comparable to standard, are CA3, CA6, CA9, CA10, C7, BS1, BS4, and PS4 but these were not considered for discussion due to their poor experimental r^2 values. The remaining analogs, which were active at very high concentrations in the protease inhibition assay, did not show interaction with the catalytic triad, which might be the reason for their inactivity.

It was also noted that when the aromatic ring was attached/fused with additional heterocyclic ring it reflected a higher activity, as observed with benzimidazole analogs showing better IC₅₀ values. Whereas, increasing the chain length for synergistic activity as in case of linkage analogs, did not show any additional benefit. It was pragmatic that, the analogs, which interacted with all the triad residues, showed better IC₅₀ values.

Fig. 5 Plot of % DENV2 NS2B/NS3pro inhibition vs. log concentration of standard quercetin (a), CA2 (b), BZ1 (c), BS2 (d), and overlay of quercetin and CA2 (e)



Conclusion

The severity of dengue infection is increasing day by day and the unavailability of specific medication is making the scenario more unmanageable. Many scientists across the globe are continuously contributing their knowledge to give a breakthrough in the treatment of DENV. Our studies in the lead optimization focused on the natural phytoconstituents, designing the analogs by considering the important structural features, and develop a promising NS2B-NS3 protease inhibitor. In computational studies, we found most of the designed analogs showed interaction with the triad residues of the enzyme, in a similar manner as that of reported phytoconstituents. Among all the designed analogs, benzimidazole and

cinnamic acid analogs showed better IC_{50} value and more potency in protease inhibition compared to that of standard quercetin [13–17].

Acknowledgements MAK acknowledges Indian Council of Medical Research (ICMR), New Delhi (58/27/2007-BMS) for computational facility and Department of Science and Technology (DST-FIST), New Delhi (SR/FST/College-264/2015(C)) for spectroscopic facility at Prin K M Kundnani College of Pharmacy, Mumbai. LRG acknowledges National NMR Facility provided by Tata Institute of Fundamental Research (TIFR), Colaba, Mumbai.

Compliance with ethical standards

Conflict of interest The authors declare that they have no conflict of interest.

Ethical approval This article does not contain any studies with human participants or animals performed by any of the authors.

Publisher's note Springer Nature remains neutral with regard to jurisdictional claims in published maps and institutional affiliations.

References

1. Wangikar P, Martis EAF, Ambre PK, Nandan S, Coutinho EC. Update on methyltransferase inhibitors of the dengue virus and further scope in the field. *J Emerg Infect Dis*. 2016;1:1–10. <https://doi.org/10.4172/2472-4998.1000108>.
2. Chambers TJ, Nestorowicz A, Amberg SM, Rice CM. Mutagenesis of the yellow fever virus NS2B protein: effects on proteolytic processing, NS2B-NS3 complex formation, and viral replication. *J Virol*. 1993;67:6797–807.
3. Wu CF, Wang SH, Sun CM, Hu ST, Syu WJ. Activation of dengue protease autocleavage at the NS2B-NS3 junction by recombinant NS3 and GST-NS2B fusion proteins. *J Virol Methods*. 2003;114:45–54. <https://doi.org/10.1016/j.jviromet.2003.09.001>.
4. Falgout B, Pethel M, Zhang YM, Lai CJ. Both nonstructural proteins NS2B and NS3 are required for the proteolytic processing of dengue virus nonstructural proteins. *J Virol*. 1991;65:2467–75.
5. Nisar A. Dengue fever treatment with Carica papaya leaves extracts. *Asian Pac. J Trop Biomed*. 2011;1:330–3. [https://doi.org/10.1016/S2221-1691\(11\)60055-5](https://doi.org/10.1016/S2221-1691(11)60055-5).
6. Padmanaban S, Pandian L, Kalavathi MK, Rayapadi S, Parimelzaghan A, Susmita B, et al. Flavonoid from Carica papaya inhibits NS2B-NS3 protease and prevents Dengue 2 viral assembly. *Bioinformation*. 2013;9:889–95. <https://doi.org/10.6026/97320630009889>.
7. Lai H. Design, synthesis and characterization of novel 1,2-benzisothiazole-3(2H)-one and 1,3,4-oxadiazole hybrid derivatives: Potent inhibitors of Dengue and West Nile virus NS2B/NS3 proteases. *Bioorg Med Chem*. 2013;21:102–13. <https://doi.org/10.1016/j.bmc.2012.10.058>.
8. Christoph N, Verena NS, Mira AMB, Anil K, Ralf B, Christian DK. Thiazolidinone–peptide hybrids as dengue virus protease inhibitors with antiviral activity in cell culture. *J Med Chem*. 2013;56:8389–403. <https://doi.org/10.1021/jm400828u>.
9. Isabella PG, William GL, Moacyr CJ, Ricardo JA, Jaqueline MSF. Docking and QM/MM studies of NS2B-NS3pro Inhibitors: a molecular target against the dengue virus. *J Braz Chem*. 2017;28:895–906. <https://doi.org/10.21577/0103-5053.20160242>.
10. Paul E, Nikolaus S, Allan D, Martin R, Markus K, et al. Structural basis for the activation of flaviviral NS3 proteases from dengue and West Nile virus. *Nat Struct Mol Biol Brief Commun*. 2006;13:372–3. <https://doi.org/10.1038/nsmb1073>.
11. Mosmann T. Rapid colorimetric assay for cellular growth and survival: application to proliferation and cytotoxicity assays. *J Immunol Methods*. 1983;65:55–63. [https://doi.org/10.1016/0022-1759\(83\)90303-4](https://doi.org/10.1016/0022-1759(83)90303-4).
12. Ganji LV, Kanyalkar MA. Non-structural proteases as a target of dengue virus. *J Antivir Antiretrovir*. 2019;11:1–15. <https://doi.org/10.35248/1948-5964.19.11.188>.
13. Raut R, Beesetti H, Tyagi P, Khanna I, Jain SK, Jeankumar VU, et al. A small molecule inhibitor of dengue virus type 2 protease inhibits the replication of all four dengue virus serotypes in cell culture. *Virology*. 2015;12:1–7. <https://doi.org/10.1186/s12985-015-0248-x>.
14. Chimera interface to modeller. UCSF Computer Graphics Laboratory; 2015.
15. San Diego: Discovery Studio, 3.1, Accelrys Inc.
16. Duan Y, Wu C, Chowdhury S, Lee MC, Xiaong G, et al. Point-charge force field for molecular mechanics simulations of proteins based on condensed-phase quantum mechanical calculations. *J Comput Chem*. 2003;24:1999–2012. <https://doi.org/10.1002/jcc.10349>.
17. Laskowski RA, MacArthur MW, Moss DS, Thornton JM. PROCHECK: a program to check the stereochemical quality of protein structures. *J Appl Cryst*. 1993;26:283–91. <https://doi.org/10.1107/S0021889892009944>.